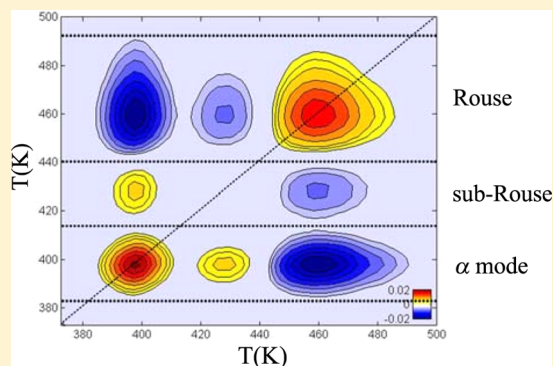


Quantifying Changes in the Low-Frequency Dynamics of Amorphous Polymers by 2D Correlation Mechanical Spectroscopy

Xuebang Wu,* Huaguang Wang, Zhengang Zhu, and C. S. Liu*

Key Laboratory of Materials Physics, Institute of Solid State Physics, Chinese Academy of Sciences, P.O. Box 1129, Hefei 230031, P. R. China

ABSTRACT: The longer segmental dynamics of sub-Rouse modes in polystyrene with different molecular weights has been investigated by 2D correlation mechanical spectroscopy. The sub-Rouse modes were first separated from the α relaxation and Rouse modes, and their dynamics exhibits a similar change at the same temperature, $T_B \approx 1.2T_g$, as the α relaxation. The relaxation time of sub-Rouse modes at T_B is independent of molecular weight and has a value of about 0.1 s, indicating that solely the time scale of the relaxation determines the change in dynamics of sub-Rouse modes. According to the coupling model, the change is caused by a strong increase in intermolecular cooperativity. The present work provides direct evidence for the intermolecular coupled nature of the sub-Rouse modes and demonstrates that the properties of the sub-Rouse modes resemble those of α relaxation, which could provide a new perspective for understanding the glass transition of polymers.



INTRODUCTION

Relaxation processes of amorphous polymers are an important concern because they govern their macroscopic mechanical behavior. Hence, the detailed analysis of these relaxation processes and their origin on a molecular scale have been subjects of interest in the past several years.^{1–4} Depending on the temperature, relaxations of various length scales in polymers take place at various times. Local motions within a chain are secondary β relaxation. The local segmental (α) relaxation, a cooperative motion of repeat units from polymer chains, is enthalpic and determines the glass transition. Rouse modes, based on the motions of Gaussian submolecules formed by sufficient numbers of repeat units in each chain, are entropic in nature and dominate the viscoelastic response in the glass–rubber region.^{5,6} Rouse dynamics occurs over a length scale shorter than that associated with topological interactions (entanglements) but involves chain segments sufficient long to be Gaussian submolecules. It has been suggested that these chain segments contain on the order of 50 or more backbonds. Furthermore, sub-Rouse modes, another type of relaxation mode that is immediate in both time and length scales between α relaxation and Rouse modes, were also observed in some polymers in the glass-to-rubber transition zone, also referred to as the softening dispersion.^{7–10} The relaxation units of sub-Rouse modes involve backbone bonds on the order of 10, which are larger than the local segmental relaxation, but smaller than the Gaussian submolecules that are the basis unit of Rouse modes. The motion of the sub-Rouse modes is slower than local segmental motion because of the longer length scale of motion but still faster than the entropically driven Rouse modes. Donth et al.^{11,12} also divided the softening dispersion region into three zones, namely, proper glass transition,

confined flow, and hindering zone, corresponding to local segmental motion, sub-Rouse modes, and Rouse modes, respectively.

For the first time, sub-Rouse modes were found in polyisobutylene (PIB) together with α relaxation by photon correlation spectroscopy^{8,13} and together with Rouse modes by creep compliance and dynamic mechanical relaxation.⁶ This polymer was chosen because it has a very broad glass–rubber transition zone, which makes it easier to resolve the sub-Rouse modes from the α relaxation and the Rouse modes. Recent results show that the sub-Rouse modes can also be resolved in some other polymers by inverted torsion pendulum and dielectric probes.^{10,14–19} Furthermore, by using two-dimensional (2D) correlation analysis, Wang et al. were able to discern the sub-Rouse modes in type-B polymers from the α relaxation and the Rouse modes.^{20,21} However, these results have not shed more light on the properties and viscoelastic mechanism of the sub-Rouse modes. In this work, by separating the sub-Rouse modes from the other two modes using 2D correlation mechanical spectroscopy, the molecular relaxation dynamics of the sub-Rouse modes in polystyrene (PS) with different molecular weights (MWs) has been investigated. It was found that the sub-Rouse modes are cooperative in nature and their dynamics is determined solely by the time scale of the relaxation, which provides new insight into the relaxation dynamics of polymers during softening dispersion.

Received: November 27, 2012

Revised: December 12, 2012

Published: December 12, 2012

EXPERIMENTAL SECTION

Materials. Monodisperse PS samples, characterized by $3.0 \leq M_w \leq 110$ kg/mol and $M_w/M_n \leq 1.05$, were prepared by anionic polymerization. The characterization of the samples is listed in Table 1. The PS samples were prepared by anionic

Table 1. Molecular Weights of the Samples Studied^a

name ^b	M_w (g/mol)	M_w/M_n	T_g (K)
PS3000	3000	1.09	330
PS6000	6000	1.05	351
PS14000	14000	1.03	362
PS20000	20000	1.02	366
PS27000	27000	1.03	374
PS42000	42000	1.05	375
PS88000	88000	1.10	376
PS110000	110000	1.01	377

^a M_w , weight-average molecular weight; M_w/M_n , polydispersity; T_g , glass transition temperature. ^bSample name indicates M_w .

polymerization in tetrahydrofuran (THF) with *n*-butyllithium as the initiator at a temperature of ~ 351 K under a pressure of $< 10^{-6}$ mm. The molecular weights and polydispersities were estimated by gel permeation chromatography (GPC) on a Waters 1515 instrument using polystyrene as a standard. The glass transition temperature was measured by differential scanning calorimetry (DSC) using a Perkin-Elmer instrument at a heating rate of 10 K/min. Prior to the mechanical spectroscopy measurements, all samples were dried under a vacuum to remove water, solvent, and residual monomer.

Measurements and Characterization. Measurements of the shear mechanical losses of the samples were made by using a modified low-frequency inverted torsion pendulum with a Couette-like setup using the forced-vibration method. A detailed description of the apparatus and procedure can be found elsewhere.¹⁵ The isothermal loss tangent $\tan \delta$, storage modulus G' , and loss modulus G'' were measured over a frequency (f) range from 5×10^{-3} to 100 Hz at constant temperature. These isothermal measurements were first carried out at some low temperature and thereafter at higher temperatures incremented by small steps. Isochronal measurements of $\tan \delta$, G' , and G'' were also made for samples during the cooling process at fixed frequencies of 0.05, 0.5, 2.0, and 8.0 Hz.

Two-Dimensional Correlation Analysis of Mechanical Spectra. Generalized 2D correlation spectroscopy was originally proposed to study the spectral intensity fluctuations under certain environmental perturbations.^{22,23} Since then, 2D correlation analysis has been expanded to various spectroscopic techniques including NMR, IR, Raman, and dielectric spectroscopies,^{20–26} which have been applied to study molecular dynamics where an exact identification of relaxation mechanisms with different time scales is always the key goal. In the present study, the 2D correlation mechanical spectra were processed and calculated by a homemade program of Matlab (Mathworks, Natick, MA), which can be used to improve the resolution by spreading the band peaks along the second spectral dimension from the heavily overlapped 1D spectra. A detailed description of the theory can be found elsewhere.^{20,21} The 2D synchronous correlation intensity can be obtained from mechanical spectra by

$$\Phi(v_1, v_2) = \frac{1}{T_{\max} - T_{\min}} \int_{T_{\min}}^{T_{\max}} \tilde{y}(v_1, t) \tilde{y}(v_2, t) dt \quad (1)$$

where $\tilde{y}(v, t)$ refers to “dynamic spectra” at temperature t ($T_{\min} \leq t \leq T_{\max}$), calculated as

$$\tilde{y}(v, t) = y(v, t) - \frac{1}{T_{\max} - T_{\min}} \int_{T_{\min}}^{T_{\max}} y(v, t) dt \quad (2)$$

where $y(v, t)$ is the mechanical intensity at frequency v and temperature t . The 2D spectrum describes the variance of a spectral intensity change induced by an external parameter, which is usually wavelength, scattering angle, frequency, and so on. In the present study, however, the treatment with temperature and frequency as the primary variables is unusual.

RESULTS AND DISCUSSION

The loss tangent, $\tan \delta$, is an alternative to the storage modulus G' and loss modulus G'' to characterize the material viscoelasticity. For some viscoelastic mechanism, $\tan \delta$ is more prominent and sensitive to changes in temperature in isochronal measurement and in frequency in isothermal measurement than G' and G'' . This is the case for modes of relaxation involving motion of longer scales such as the sub-Rouse modes and Rouse modes. On the other hand, the local segmental relaxation shows up more favorably as loss peaks when mechanical data are presented by G'' .^{11,27} The isochronal mechanical spectra given in terms of $\tan \delta$, G' and G'' of PS with $M_w = 88$ kg/mol at different frequencies are shown in Figure 1 at the temperature range of 350–510 K. The loss

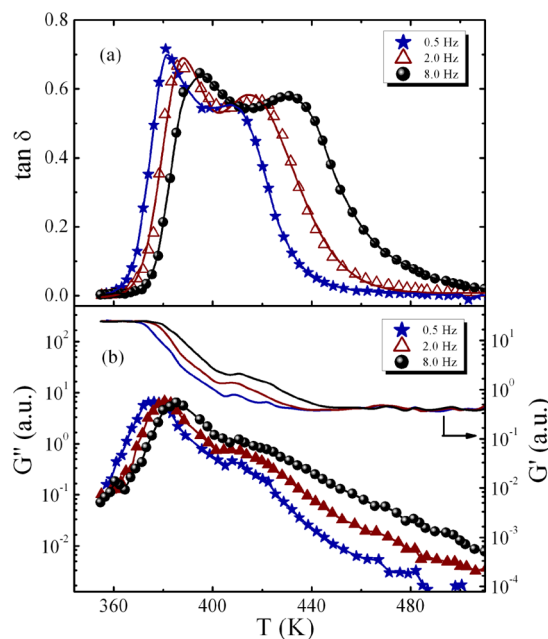


Figure 1. (a) $\tan \delta$ and (b) G' and G'' versus temperature for PS with $M_w = 88$ kg/mol at 0.5, 2.0, and 8.0 Hz.

tangent of PS exhibits an asymmetric double-peak structure. With the appearance of the lower temperature peak, G' exhibits a sharp decrease and G'' shows a maximum. It is well-known that a strong decay of G' occurs during the glass transition and at the same time G'' (and also $\tan \delta$) displays a maximum.²⁸ Moreover, the value of T_g corresponds to the temperature at which the segmental relaxation time becomes the time scale of

DSC measurements, namely 100 s ($f = 1/(2\pi\tau) \approx 10^{-3}$ Hz).^{29–32} The lower temperature G'' peak at a very low frequency is located approximately at T_g determined by DSC measurements. So it is reasonable to attribute the lower temperature $\tan \delta$ peak to the faster α process. Naturally the higher temperature $\tan \delta$ peak is associated with motion of more repeat units in each chain than the α process.

The isochronal mechanical loss tangent spectra of PS with different MWs are shown in Figure 2 at 2.0 Hz. As shown, all

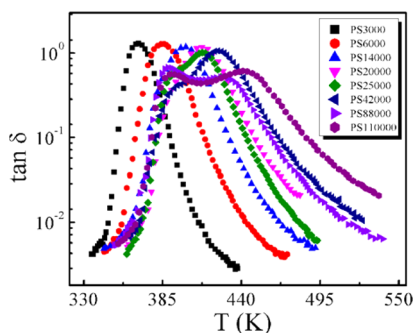


Figure 2. Isochronal mechanical loss tangent spectra of PS with different MWs at 2.0 Hz.

samples exhibited an asymmetric double-peak structure. The outstanding feature in Figure 2 is the trend of the variation of $\tan \delta$ with MW. With increasing chain lengths, both the α process and the slow relaxation move to higher temperatures mainly because of an increase in T_g . Furthermore, for PS with high MW, both of the processes are clearly observed over a large temperature and frequency range. The lower the MW, the smaller the separation between the two relaxations. Hence, with decreasing MW, the α peak becomes almost submerged under the maximum peak. The merging of the α process and the slow relaxation with decreasing MW indicates strong coupling between the two modes. This is understandable because the relaxation units of both the α motion and the slow relaxation are close to each other with decreasing MW.

Because of the overlap and coupling of different molecular modes in Figures 1 and 2, it is difficult to resolve the contribution of each mode and gain more useful information from 1D loss tangent spectra. With the help of 2D correlation analysis, synchronous spectra can be obtained, as shown in Figure 3a. The synchronous 2D correlation spectra show a simultaneous change of two peaks, where the red-colored regions are defined as the positive correlation intensities and the blue-colored regions are regarded as the negative correlation intensities.^{20,21} The synchronous spectra are symmetric with respect to the diagonal line. The peaks located along the diagonal line are called autopeaks and are always positive, whereas those located at off-diagonal positions are called crosspeaks and will be positive if the intensity variations of the two peaks occur in the same direction (the intensities of corresponding peaks in 1D spectra both increase or decrease) or negative otherwise. Surprisingly, although only two peaks (the shoulder and the maximum) can be found in Figures 1 and 2, three peaks appear in Figure 3a, which indeed verifies the high resolution of 2D correlation analysis. Compared with Figure 3b, the crosspeak at (383, 410) K and the autopeak at (410, 410) K are assigned to the shoulder and the maximum, respectively, of the $\tan \delta$ peak. As mentioned above, the shoulder is related to the faster α process, whereas the

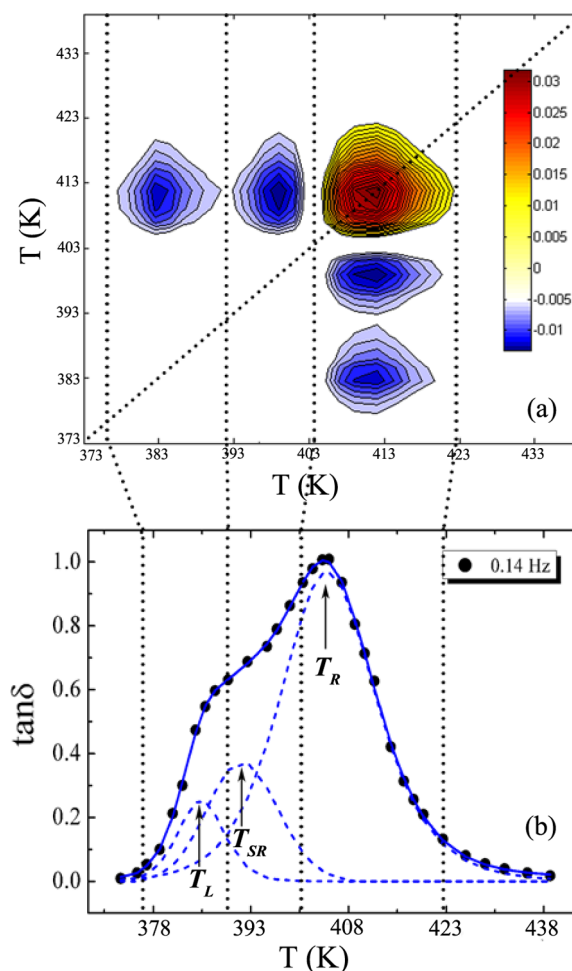


Figure 3. (a) Synchronous 2D correlation mechanical spectrum of PS with $M_w = 27$ kg/mol in the temperature range of 373–450 K (red region, positive; blue region, negative). (b) According to the results of 2D correlation analysis, the asymmetric loss tangent spectrum at 0.14 Hz of PS can be resolved into three peaks (dotted blue lines) using a nonlinear fitting method, corresponding to local segmental motion, sub-Rouse modes, and Rouse modes.

maximum is ascribed to a slow process such as the Rouse modes. Therefore, the crosspeak at (398, 410) K, which is located between (383, 410) and (410, 410) K, should be referred to the motions intermediate in length and time scales to the α relaxation and Rouse modes. Following the nomenclature proposed by Santangelo et al.,²⁹ the relaxation mode is assigned to sub-Rouse relaxation, involving on the order of ~ 10 backbone bonds. This successful and direct separation of three heavily overlapped modes of molecular motions reveals the remarkable advantages of 2D correlation analysis for studying molecular dynamics. On the basis of the positions and widths of the autopeaks and crosspeaks, the asymmetrical loss peak can be decomposed by the nonlinear fitting method.³³ Assuming that the peak function is a Debye function with a log-normal distribution in the relaxation time, the total temperature-dependent function of $\tan \delta$ is the linear composition of one or more Debye peaks described as

$$\tan \delta(T) = \frac{1}{2\sqrt{\pi}} \sum_{i=1}^M \Delta_i \int_{-\infty}^{+\infty} \exp(-w^2) \operatorname{sech}(x_i + \beta_i w) dw + \tan \delta(T_c) \quad (3)$$

where M is the number of peaks, $x_i = \ln(\omega\tau_{mi})$, $\omega = 2\pi f$, τ_{mi} is the most probable relaxation time of the i th relaxation process (the i th peak), w is the integrating variable, $\tan \delta(T_c)$ is the background, β_i is the distribution parameter, and Δ_i is the relaxation strength of the i th peak. Note that the fitting procedures were carried out manually by changing the peak temperature, the relaxation strength, the most probable relaxation time, and the distribution parameter at one time, so the obtained fitting results have some inevitable uncertainties. In the present study, because the peak positions and the widths of the autopeaks and crosspeaks for three modes were determined by the 2D correlation analysis, the $\tan \delta$ spectrum can be well resolved into three peaks by the nonlinear fitting procedure shown in Figure 3b, corresponding to local segmental mode, sub-Rouse modes, and Rouse modes.

As described above, the G'' peak mainly reflects the motion of local segments, whereas the $\tan \delta$ peak mainly reflects the sub-Rouse modes and Rouse modes.^{11,27} This could also be confirmed by measurements of frequency-domain mechanical spectra. Figure 4 shows the isothermal mechanical spectra of

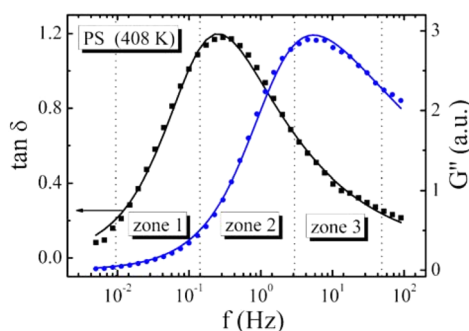


Figure 4. Isothermal mechanical spectra of $\tan \delta$ (squares) and G'' (circles) of PS20000 at 408 K. Similarly to the results of Donth et al.,^{11,12} the main transition can be divided into three zones, namely, local segmental motion (zone 3), sub-Rouse modes (zone 2), and Rouse modes (zone 1).

$\tan \delta$ and loss modulus G'' of PS20000 at 408 K. Similarly to the findings of Donth et al.,^{11,12} the main transition can be divided into three $\log f$ ranges that are called zones, namely, local segmental motion (zone 3), sub-Rouse modes (zone 2), and Rouse modes (zone 1). Note that the relaxation behaviors presented by G'' in zones 1 and 2 are not obvious compared to that presented by $\tan \delta$, so the dynamics of the sub-Rouse and Rouse modes can be obtained by the analysis of $\tan \delta$ peak in zones 1 and 2.

To gain a better insight into the dynamics of the sub-Rouse modes, the frequency-domain spectra of PS27000 were transformed into a 2D correlation spectrum based on autocorrelation calculations in the frequency range of $10^{-2.5}$ – 10^2 Hz, as shown in Figure 5a. Figure 5b is the corresponding $\tan \delta$ curve. Compared with Figure 5b, the positive autopeak at $(10^{-1.7}, 10^{-1.7})$ Hz is identified with α relaxation. The negative crosspeak at $(10^{1.4}, 10^{-1.7})$ Hz, appearing to be much slower than α relaxation, should be assigned to the Rouse modes. Naturally, the crosspeak at $(10^{-0.6}, 10^{-1.7})$ Hz, which is located between $(10^{-1.7}, 10^{-1.7})$ and $(10^{1.4}, 10^{-1.7})$ Hz, should be ascribed to the sub-Rouse modes with motions intermediate in length and time scale between the α relaxation and the Rouse modes. Based on the peak positions and the widths of the three modes determined by the 2D correlation analysis, the spectra

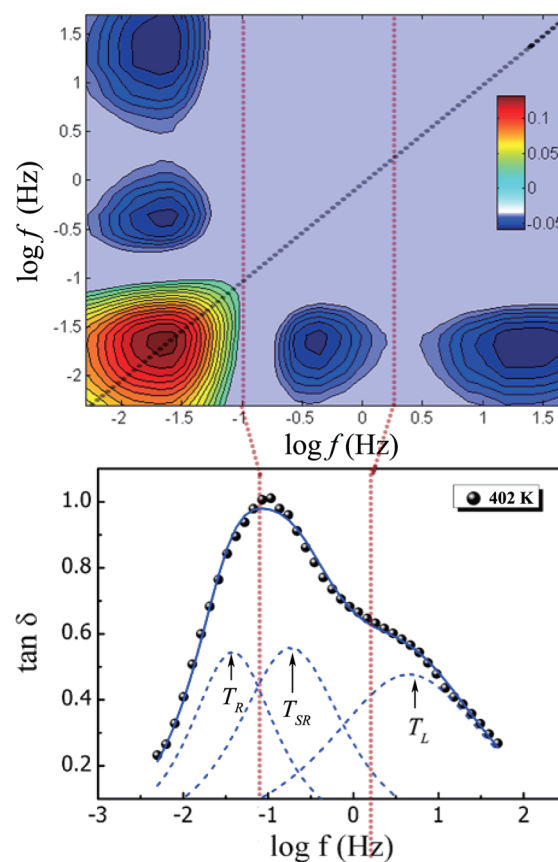


Figure 5. (a) Synchronous 2D correlation mechanical spectrum of PS with $M_w = 27$ kg/mol in the frequency range of $10^{-2.5}$ – 10^2 Hz (red region, positive; blue region, negative). (b) According to the results of 2D correlation analysis, the $\tan \delta$ spectrum of PS at 402 K can be fitted by additive contributions of three HN functions, corresponding to local segmental motion, sub-Rouse modes, and Rouse modes.

were fitted by additive contributions of three Haviliak–Negami (HN) functions for G'' and $\tan \delta$ according to

$$G'' = \sum_{i=1,2,3} \Delta_i / [1 + (i\omega\tau_i)^2]^{\lambda_i/\gamma_i} \quad (4)$$

where Δ_i is the relaxation strength and λ_i and γ_i are fractions of unity. From the fits, the relaxation time and frequency dispersion of the sub-Rouse modes were obtained as a function of temperature. As an example, the three HN functions that fit the $\tan \delta$ peak of PS27000 at 402 K are shown in Figure 5b.

In Figure 6 are plotted the temperature dependence of characteristic relaxation time τ of the sub-Rouse modes for PS with different MWs. A close examination of data over a wide temperature range where the sub-Rouse modes occur reveals that the $\tau(T)$ dependence cannot be described accurately by a single Vogel–Fulcher–Tammann (VFT) equation over the entire temperature range, as shown by dashed lines in Figure 6. Two VFT equations are required to fit the data for PS. This was confirmed using the method proposed by Stickel and co-workers,³⁴ whereby the $\tau(T)$ data are transformed into $\phi_T = \{-d \log[\tau(T)/dT]\}^{-1/2}$ as a function of T . Note that the derivative in the Stickel plots is highly accurate because the temperature data (~ 4 K) are sufficiently finely spaced. The crossover of $\tau(T)$ from one VFT law to another is confirmed by the fact that ϕ_T exhibits a change in slope at some characteristic temperature T_B (inset in Figure 6). The values of T_B increase

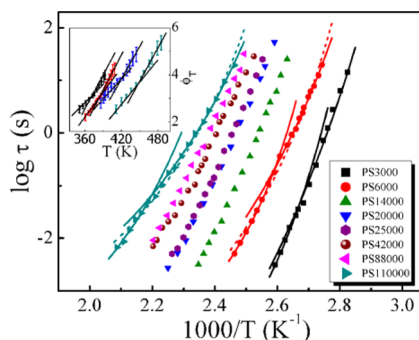


Figure 6. Temperature dependence of relaxation time of the sub-Rouse modes for PS with different MWs. Two VFT equations are required to describe the relaxation behaviors of PS above T_g . The solid lines represent the two VFTs for the polymers, and a crossover is clearly seen. The dashed lines correspond to the fits by a single VFT equation. The inset shows plots of the Stickel function, $\phi_T = \{-d \log[\tau(T)]/dT\}^{-1/2}$, against temperature for PS3000, PS6000, PS20000, and PS110000. The crossover temperature T_B was estimated from the intersection of two straight lines.

with increasing MW, but the T_B/T_g ratios decrease, which is similar to the behavior for the dynamics of α relaxation in polymers.^{35–37} However, the crossover relaxation time is almost the same for the polymers: $\tau(T_B) = 0.1$ s, independent of MW.

It is known that the dynamics of α relaxation in amorphous polymers exhibits a crossover at $\sim 1.2T_g$ and that the crossover relaxation time is almost the same for amorphous polymers, being $\tau(T_B) = 10^{-7} - 10^{-6}$ s, independent of MW and molecular structure as well as applied pressure.^{36,38} The change in dynamics seems to be related to some critical relaxation time at which the dynamics of glass-forming liquids crosses over from a liquid-like behavior to a solid-like behavior on a molecular scale. Here, we found that the crossover in dynamics of the sub-Rouse modes and the α relaxation appears to occur at approximately the same temperature: $T_B \approx 1.2T_g$. The variation in MW, as well as the blend compositions in the previous work,¹⁶ has no significant influence on the crossover relaxation time at T_B . This fact demonstrates that the time scale of the relaxation is the most important parameter governing the change in dynamics for the sub-Rouse modes. This crossover arises not at some critical temperature, but rather at a particular value of the relaxation time, which is again another characteristic of the change in dynamics of the structural relaxation of low-molecular-weight glass formers at T_B .^{39,40} It is generally accepted that the structural and segmental relaxation time for molecular liquids and polymers is invariant to thermodynamic conditions at various dynamic “transitions”.³⁸ If the origin of this phenomenon found for sub-Rouse modes is the same as local segmental relaxation or structural relaxation in the case of low-molecular-weight glass formers,⁴¹ then the crossover of $\tau(T)$ is caused by a change in intermolecular coupling at T_B .

The crossover behavior of $\tau(T)$ is also visible in the temperature dependence of the frequency dispersion of the sub-Rouse modes. The only theoretical model for relating frequency dispersion to dynamics of relaxation processes is the coupling model (CM), which identifies the broadening of the relaxation peak as being due to intermolecular coupling.^{8,42,43} In the CM, the broadening or degree of departure from exponential decay is measured by the coupling parameter, n ,

appearing in the exponent of the Kohlrausch–William–Watts function

$$\varphi(t) = \exp[-(t/\tau)^{(1-n)}] \quad (5)$$

whereas n is related to w , the full-width at half-maximum of the loss peak normalized to that of the Debye relaxation, by the relation $n = 1.041(1 - w^{-1})$.^{35,44} The parameter n ($0 \leq n < 1$) increases with increasing intermolecular interaction. The temperature dependence of n is a direct indication of how intermolecular coupling strength changes with temperature. Because the parameter n is equivalent to $(1 - \beta_{\text{KWW}})$ and $\beta_{\text{KWW}} = (\lambda\gamma)^{1/1.23}$ for an HN function,⁴⁵ the value of n for the sub-Rouse modes can be obtained. In Figure 7, we plot the

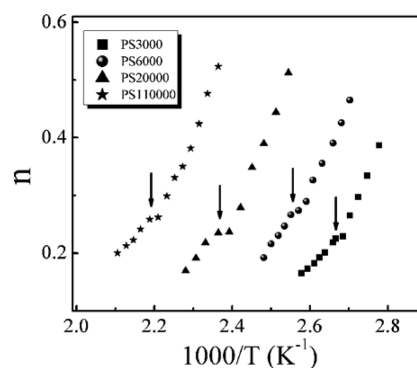


Figure 7. Temperature dependence of the coupling parameter n for PS with different MWs.

temperature dependence of the coupling parameter of the sub-Rouse modes for PS with different MWs. It can be seen that, with decreasing temperature, $n(T)$ crosses over at T_B from slowly varying and small values of $n(T)$ to a more rapidly increasing values of $n(T)$. The increase of $n(T)$ is monotonic, and $n(T)$ reaches a large value on approaching T_g . Therefore, the crossover phenomenon of $n(T)$ and $\tau(T_B)$ seems to be general and is apparently due to the change in the intermolecular coupling of the sub-Rouse modes at T_B , analogous to that found in the α relaxation and structural relaxation in the case of low-molecular-weight glass formers. Moreover, it can be seen from Figure 7 that the value of $n(T)$ seems to be dependent on MW, and at a given temperature, $n(T)$ decreases with decreasing MW, which agrees well with the results of Ngai et al.⁴² With decreasing MW, the concentration of chain ends increases, leading to a higher mobility. In the CM, the presence of a more mobile component reduces the coupling parameter n of the other component. Thus, a polymer with lower MW will have a smaller value of n .⁴²

It has been argued that the slow process was caused by a third-order thermodynamic transition from one liquid state to another with the breakup of localized order,⁴⁶ but it was refuted by Plazek, who showed that there is an absence of transition in the softening dispersion zone.⁴⁷ The proper interpretation of the slow mode is a longer-scale segmental relaxation composed of the sub-Rouse modes and Rouse modes.^{15–17} The present results further confirm the existence of sub-Rouse modes and Rouse modes at frequencies below α relaxation and that there is no thermodynamic transition in the glass-to-rubber transition zone. The only change is the change in dynamics of the sub-Rouse modes when crossing T_B due to the marked increase in the degree of intermolecular cooperativity with falling temperature, similar to that found for the dynamics of α relaxation.

Naturally, because the sub-Rouse modes are much slower than the local segmental mode, the crossover relaxation time $\tau(T_B)$ of the sub-Rouse modes is much longer than that of the local segmental mode.

CONCLUSIONS

In conclusion, using 2D correlation mechanical spectroscopy, the sub-Rouse modes of polystyrene were first separated from the α relaxation and the Rouse modes. The dynamics of the sub-Rouse modes exhibit a crossover at T_B similar to that of the α relaxation and structural relaxation in the case of low-molecular-weight glass formers. The crossover relaxation time of the sub-Rouse modes at T_B is almost the same for all of the polymers investigated, that is, $\tau(T_B) = 0.1$ s, independent of molecular weight. Using the coupling model for interpretation, the crossover is suggested to be due to a change in the strength of intermolecular coupling when crossing T_B , in the same manner as used by others to interpret the similar change of dynamics of structural relaxation. The results suggest that the sub-Rouse modes and the dynamic crossover they exhibit can generally be found in polymers by 2D correlation mechanical spectroscopy.

AUTHOR INFORMATION

Corresponding Author

*E-mail: xbwu@issp.ac.cn (X.W.), cslu@issp.ac.cn (C.S.L.).

Notes

The authors declare no competing financial interest.

ACKNOWLEDGMENTS

This work was supported by the National Natural Science Foundation of China (11174283, 11074253, and 50803066).

REFERENCES

- (1) Munch, E.; Pelletier, J. M.; Sixou, B.; Vigier, G. *Phys. Rev. Lett.* **2006**, *97*, 207801.
- (2) Sokolov, A. P.; Schweizer, K. S. *Phys. Rev. Lett.* **2009**, *102*, 248301.
- (3) Ngai, K. L.; Plazek, D. J.; Roland, C. M. *Phys. Rev. Lett.* **2009**, *103*, 159801.
- (4) Schwabe, M.; Rotzoll, R.; Kuchemann, S.; Nadimpalli, K.; Vana, P.; Samwer, K. *Macromol. Chem. Phys.* **2010**, *211*, 1673–1677.
- (5) Ferry, D. J. *Viscoelastic Properties of Polymers*, 3rd ed.; Wiley: New York, 1980.
- (6) Plazek, D. J.; Chay, I. C.; Ngai, K. L.; Roland, C. M. *Macromolecules* **1995**, *28*, 6432–6436.
- (7) Santangelo, P. G.; Ngai, K. L.; Roland, C. M. *Macromolecules* **1993**, *26*, 2682–2687.
- (8) Ngai, K. L.; Plazek, D. J.; Rizos, A. K. *J. Polym. Sci. B: Polym. Phys.* **1997**, *35*, 599–614.
- (9) Ngai, K. L.; Plazek, D. J.; Rendell, R. W. *Rheol. Acta* **1997**, *36*, 307–319.
- (10) Paluch, M.; Pawlus, S.; Sokolov, A. P.; Ngai, K. L. *Macromolecules* **2010**, *43*, 3103–3106.
- (11) Donth, E.; Beiner, M.; Reissig, S.; Korus, J.; Garwe, F.; Vieweg, S.; Kahle, S.; Hempel, E.; Schroter, K. *Macromolecules* **1996**, *29*, 6589–6600.
- (12) Reissig, S.; Beiner, M.; Vieweg, S.; Schroter, K.; Donth, E. *Macromolecules* **1996**, *29*, 3996–3999.
- (13) Rizos, A. K.; Jian, T.; Ngai, K. L. *Macromolecules* **1995**, *28*, 517–521.
- (14) Wu, X. B.; Zhou, X. M.; Liu, C. S.; Zhu, Z. G. *J. Appl. Phys.* **2009**, *106*, 013527.
- (15) Wu, X. B.; Zhu, Z. G. *J. Phys. Chem. B* **2009**, *113*, 11147–11152.

- (16) Wu, X. B.; Wang, H. G.; Liu, C. S.; Zhu, Z. G. *Soft Matter* **2011**, *7*, 579–586.
- (17) Wu, X. B.; Liu, C. S.; Zhu, Z. G.; Ngai, K. L.; Wang, L. M. *Macromolecules* **2011**, *44*, 3605–3610.
- (18) Wu, J. R.; Huang, G. S.; Pan, Q. Y.; Qu, L. L.; Zhu, Y. C.; Wang, B. *Appl. Phys. Lett.* **2006**, *89*, 121904.
- (19) Wu, J. R.; Huang, G. S.; Wang, X. A.; He, X. J.; Zheng, J. *Soft Matter* **2011**, *7*, 9224–9230.
- (20) Wang, X.; Huang, G. S.; Wu, J. R.; Nie, Y. J.; He, X. J. *J. Phys. Chem. B* **2011**, *115*, 1775–1779.
- (21) Wang, X. A.; Huang, G. S.; Wu, J. R.; Nie, Y. J.; He, X. J.; Xiang, K. W. *Appl. Phys. Lett.* **2011**, *99*, 121902.
- (22) Noda, I. *Appl. Spectrosc.* **1993**, *47*, 1329–1336.
- (23) Noda, I. *Appl. Spectrosc.* **2000**, *54*, 994–999.
- (24) Eads, C. D.; Noda, I. *J. Am. Chem. Soc.* **2002**, *124*, 1111–1118.
- (25) Jung, Y. M.; Czarnik-Matusewicz, B.; Ozaki, Y. *J. Phys. Chem. B* **2000**, *104*, 7812–7817.
- (26) Zhang, H.; Mijovic, J. *Macromolecules* **2004**, *37*, 5844–5846.
- (27) Ngai, K. L.; Plazek, D. J. *Rubber Chem. Technol.* **1995**, *68*, 376–434.
- (28) Pelletier, J. M.; Gauthier, C.; Chazeau, L. *Int. J. Mater. Prod. Technol.* **2006**, *26*, 312–325.
- (29) Santangelo, P. G.; Roland, C. M. *Macromolecules* **1998**, *31*, 4581–4585.
- (30) Roland, C. M.; Casalini, R. *J. Chem. Phys.* **2003**, *119*, 1838–1842.
- (31) Mandanici, A.; Shi, X. F.; McKenna, G. B.; Cutroni, M. *J. Chem. Phys.* **2005**, *122*, 114501.
- (32) Hirose, Y.; Adachi, K. *Macromolecules* **2006**, *39*, 1779–1789.
- (33) Wang, X. P.; Fang, Q. F. *J. Phys.: Condens. Matter* **2001**, *13*, 1641–1651.
- (34) Stickel, F.; Fischer, E. W.; Richert, R. *J. Chem. Phys.* **1995**, *102*, 6251–6257.
- (35) Ngai, K. L.; Roland, C. M. *Polymer* **2002**, *43*, 567–573.
- (36) Pawlus, S.; Kunal, K.; Hong, L.; Sokolov, A. P. *Polymer* **2008**, *49*, 2918–2923.
- (37) Casalini, R.; Roland, C. M.; Capaccioli, S. *J. Chem. Phys.* **2007**, *126*, 184903.
- (38) Roland, C. M. *Soft Matter* **2008**, *4*, 2316–2322.
- (39) Casalini, R.; Paluch, M.; Roland, C. M. *J. Chem. Phys.* **2003**, *118*, 5701–5703.
- (40) Casalini, R.; Roland, C. M. *Phys. Rev. B* **2005**, *71*, 014210.
- (41) Casalini, R.; Ngai, K. L.; Roland, C. M. *Phys. Rev. B* **2003**, *68*, 014201.
- (42) Ngai, K. L.; Gopalakrishnan, T. R.; Beiner, M. *Polymer* **2006**, *47*, 7222–7230.
- (43) Ngai, K. L. *Relaxation and Diffusion in Complex Systems*, 1st ed.; Springer: New York, 2011.
- (44) Dixon, P. K. *Phys. Rev. B* **1990**, *42*, 8179–8186.
- (45) Alvarez, F.; Alegria, A.; Colmenero, J. *Phys. Rev. B* **1991**, *44*, 7306.
- (46) Boyer, R. F.; Enns, J. B. *J. Appl. Polym. Sci.* **1986**, *32*, 4075–4107.
- (47) Plazek, D. J. *J. Polym. Sci. B: Polym. Phys.* **1982**, *20*, 1533–1550.